Development and experimental study of oil-free capacitor module for plasma focus device

Ravindra Kumar Sharma and Archana Sharma

Citation: Review of Scientific Instruments **88**, 033502 (2017); doi: 10.1063/1.4977218
View online: http://dx.doi.org/10.1063/1.4977218
View Table of Contents: http://aip.scitation.org/toc/rsi/88/3
Published by the American Institute of Physics

REVIEW OF SCIENTIFIC INSTRUMENTS **88**, 033502 (2017)

Development and experimental study of oil-free capacitor module for plasma focus device

Ravindra Kumar Sharma and Archana Sharma
BARC, Homi Bhabha National Institute, Mumbai 400 085, India

(Received 13 September 2016; accepted 11 February 2017; published online 3 March 2017)

This development is concerned with the compact capacitor module for a plasma focus device. Oil-free, non-standard geometry capacitors are designed and developed for high current delivery in sub-microseconds time. Metalized dielectric film based pulse capacitor becomes progressively less viable at currents above 10 kA. It is due to reliability and energy scaling difficulties, based on effects such as vaporization, high resistivity, and end connection. Bipolar electrolytic capacitors are also not preferred due to their limited life and comparatively low peak current delivery. Bi-axially oriented polypropylene (BOPP) film with extended aluminum foil is a combination to deliver moderately high power. But, electrically weak points, relative permittivity, and the edge gap margins have made its adoption difficult. A concept has been developed in lab for implementing the above combination in a less complex and costly manner. This paper concerns the development and testing process techniques for quite different hollow cylindrical, oil-free capacitors (4 μF, 10 kV, 20 nH). Shot life of 1000 has been experimentally performed on the test bed at its rated energy density level. The technological methods and engineering techniques are now available and utilized for manufacturing and testing of BOPP film based oil-free capacitors. *Published by AIP Publishing.* [http://dx.doi.org/10.1063/1.4977218]

I. INTRODUCTION

Every pulsed power system includes an energy storage device, a high voltage switch, and a load, such as the plasma focus (PF) device.[1,2] There are wide ranges of energy storage devices. These operate on various technologies: electrochemical, electrolytic, organic-inorganic material, etc. Selection of a particular type of energy module is carried out on the basis of desired discharging performances such as (a) capacitance, (b) high voltage hold-off, (c) peak current delivery capacity, (d) self inductance, and (e) number of shots (life).

Polymer film has several attributes in comparison to other materials. One of them is greater efficiency in power conversion.[3] Film capacitors have virtually no capacitance coefficient with applied voltage as observed in high permittivity ceramic capacitors. A film molecule is stable, over long-term use, and is not prone to dissipation factor, degradation, or metallic shorting mechanisms.[4]

A palm top PF device is also developed of shot life <50 shots using bipolar electrolytic capacitors.[5] Capacitor development process is a sensitive subsystem of the full pulsed power system. High energy density (0.09 J/cc) and working voltage of 100 kV have been achieved with voltage reversal (57%) and limited peak current of 200 kA.[6] In another effort, energy density and working voltage of 0.05 J/cc and 60 kV, respectively, have been achieved.[7]

High peak current with low inductance can be achieved by paralleling capacitors. This method increases component count and complexity and makes operation less reliable (high failure rate). Self inductance should be low without increasing the component count and this requires the custom design of the capacitors.[8] In order to minimize the self inductance of the capacitor, both connections must be at one end of the winding. This minimizes the magnetic field outside the capacitor winding. One option is to have a very wide winding with the return on a coaxial conductor. The inner diameter space can be utilized for the placement of the components such as triggered spark gap and PF device. Capacitor employing metalized dielectric films become progressively less viable at currents above 10 kA. It is due to reliability and energy scaling difficulties, based on effects such as vaporization, high resistivity, and end connection. Equivalent series resistance increases due to high resistivity ($\approx$50 Ω/sq) of thin metalized film and limits discharging peak current. Length of the metal sprayed end connections (10 A/m) is the limiting factor to achieve the required peak current. If a clearing/vaporization event occurs in one section of the high voltage metalized capacitor, the voltage of that section is transferred to other series section of winding. In the worst case, continuous clearing may destroy the capacitor.[9] Improvements obtained by the proposed design concepts are as follows:

(a) Oil-free capacitor design (removal of metal/plastic can).
(b) Multipoint electrical connection is a new concept between aluminum foil and disc electrodes for high current capability. This also provides lead-less (low inductance) capacitor terminals and reduction in overall size.
(c) Development of non-standard, hollow cylindrical geometry capacitor, and this is the first of its kind in pulse capacitor family.
(d) Custom design of new on-line impregnation capacitor winding machine. Weak points of the BOPP film are filled with low viscosity resin to improve voltage strength, dielectric constant and for reduction in the edge gap margin (1.5 mm/kV).

(e) Film-foil winding on polyvinyl chloride (PVC) plastic tube (inner diameter (ID): 44 mm) and utilization of inner space for return coaxial conductor is implemented first time in this manner. This helps to decrease inductance and overall size of pulsed power system.

(f) Development of oil-free, single capacitor (4 μF, 10 kV, 20 nH, 85 kA) with life of 1000 shots (without failure) against multiple capacitors in parallel.

II. DESIGN CONSIDERATION

Compact design of BOPP film and the extended aluminum foil is a combination which delivers moderately high power. This comes closest to fulfill the need as per previous discussion. Adoption of film-foil design is made difficult by its weak points (volume electrical break down), relative permittivity, and the edge gap margins to avoid the surface flash over discharge.

This requires some novel design of the on-line impregnation capacitor machine, development process techniques using low viscosity resin, and high current collection technique. Resin ($\epsilon_r = 4$) is a three part system comprising Epofine-757, Finehard-2918, and Accelerator-062 with 100:85:1 (by weight). Resin dielectric strength and volume resistivity are 22 kV/mm and $>10^{15}$ Ω cm, respectively, as per IEC 243-1.

An energy storage capacitor module (400 J) is required to generate 10^6 neutrons per discharge. Working voltage of 20 kV is used in the empirical neutron yield formula given below:

$$\text{Capacitance } (C) \text{ for energy } (E = 400\text{ J}) \text{ at } 20\text{ kV}: \ 2\ \mu\text{F},$$

$$\text{Neutron yield } (Y): \ 1.6 \times 10^6 \text{ neutrons/shot}$$

$$(Y = 10^7 \times E^2), \text{ where E is in kJ.}$$

Hollow cylindrical capacitors (4 μF, 10 kV) are developed for a PF device (2 μF, 20 kV) as shown in Figure 1.

Capacitor design consists of five layers of PP films (12 μm) between 6 μm aluminum foils as shown in Figure 2. This confirms 11 kV test voltage of the capacitor with 80% voltage reversal during discharge. Capacitance value (3.2 μF $\pm$ 10%) is calculated using parallel plate capacitor configuration before impregnation as shown in Figure 3 and Eq. (1). It is observed that the capacitance value increases by 25%-40% after resin impregnation. Capacitance values (C = 4-4.5 μF) are measured across capacitor terminals,

$$C = \varepsilon_0\ \varepsilon_r\ A / S \text{ or } C = \varepsilon_0\ \varepsilon_r\ N\ d_0\ d_l / (t_{pp}\ N_{pp}), \qquad (1)$$

where A = effective area of the aluminum foil ($\boldsymbol{d}_0 \times \mathbf{d}_l$), S = BOPP film thickness between foils ($t_{pp} \times N_{pp}$), N = number of turns in a capacitor (300 turns), d_0 = effective width of the capacitor (100 mm), d_l = length in one turn ($2 \times \Pi \times 50$ mm[mean radius]), t_{pp} = thickness of single BOPP layer (12 μm), N_{pp} = number of BOPP layers between foils (5Nos.), and $\ell/2$ = extended foil at one side of the capacitor (20 mm).

All measurements are performed using Keithley Model 3330 LCZ Meter at 1 kHz frequency. Sample capacitors (without resin) are electrically tested. These capacitors are breaking down at 70% voltage with high leakage currents compared to the same rating resin impregnated capacitors. Dielectric layer is developed at the internal edges of the aluminum foil due to

FIG. 1. Hollow cylindrical pulse capacitor 4 μF, 10 kV.

excess resin. This helps in reduction of electric field and corona formation at the foil edges. So finally reduction in edge gap (1.5 mm/kV) helps to increase the energy density of the capacitor. Cylindrical mandrel (stainless steel) is fabricated with metal key system to lock the capacitor base after insertion. PVC plastic tube (outer diameter (OD): 50 mm, ID: 44 mm, and length 155 mm) is used as a base on the mandrel and locked. This confirms zero relative motion between main mandrel and the PVC base tube. Electrical insulation is provided by the wall thickness of this PVC tube bobbin for return conductor as shown in Figure 1.

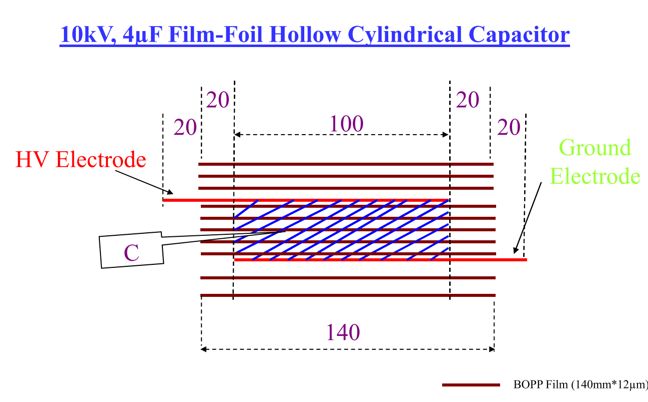

FIG. 2. Film-foil configuration for 10 kV capacitor.

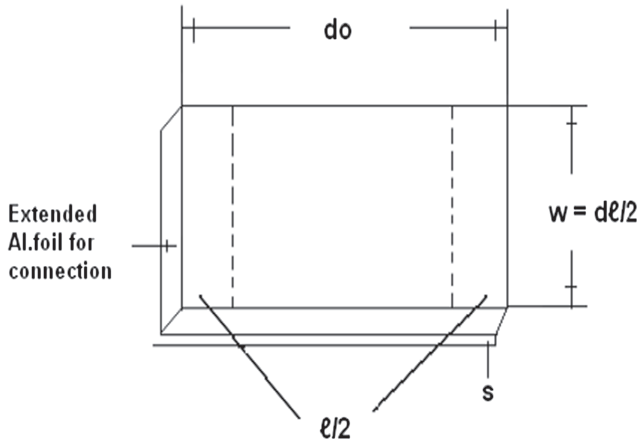

FIG. 3. Extended foil capacitor configuration.

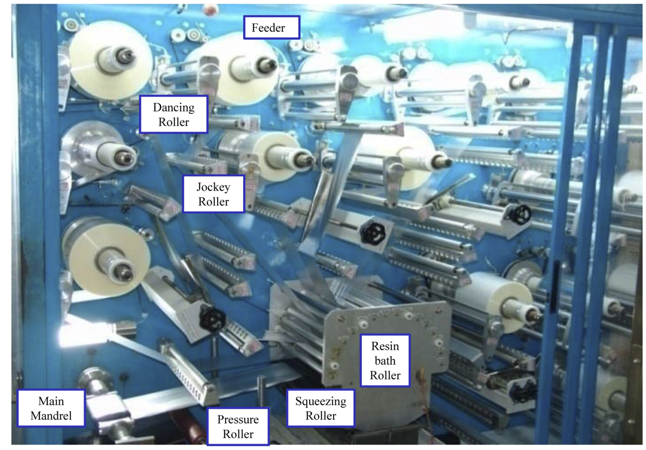

FIG. 4. On-line capacitor winding machine at Bhabha Atomic Research Centre (BARC).

It is experimentally inferred that single BOPP film thickness is increased by 2 μm after impregnation with the thermally curable resin. This film holds 400 V/μm electric field in a spring loaded experimental test setup as per ASTM D-149. Resin impregnated BOPP film is placed between spring loaded brass electrodes. Test voltage is raised at 100 V/s slope using a high voltage function generator (TREK Model 10/10B-FG).

Both side conducting surfaces (High Voltage (HV) and ground surface) are developed by 300 turns of extended film-foil configuration on PVC base as shown in Figure 2. These extended foil edges are exploited for multiple electrical point connection. This concept is employed by pressing the solid electrode disc against the foil edge's area (between ID: 50 mm to OD: 155 mm). Electrode discs (OD: 155 mm, ID: 50 mm, and thickness of 5 mm) are pressed after completion of the impregnation process. This ensures the easy entry of resin inside the capacitor element and also keeps the discs electrically connected after curing. There is not any extra length of the capacitor terminals or bushings, which needlessly increases the inductance of the capacitor element. These plates are used as main electrodes on both sides of the hollow cylindrical capacitor as shown in Figure 1. Four M3 screws are incorporated in the low inductance, one side terminal design to connect the spark gap or return coaxial conductor.[9] A concept has been developed in lab for implementing the above combination in a less complex and costly manner.

III. OIL-FREE PULSE CAPACITOR TECHNOLOGY

A special purpose on-line capacitor winding machine has been custom designed and operational to our specification. Film-foil rolls are placed on the feeders as per design configuration shown in Figure 2. These film-foils are routed through dancing roller, jockey roller, resin bath roller, squeezing roller, and pressure rollers. As per on-line definition, film-foils are dipped in resin bath and excess resin is squeezed between pressure rollers (silicon rubber) before winding at main mandrel (flat/cylindrical type) as shown in Figure 4. Extended foil capacitors are developed for pulsed power applications.[10] This same on-line capacitor winding machine is used for the development of these 4 μF, 10 kV capacitors except the placement of new cylindrical mandrel. All the operations of the capacitor winding are done manually like threading of the film-foil on the main mandrel through resin bath, initial and end foil folding, ejection of the wound capacitor from machine, placement of the resin bath in machine, etc. It is experimentally inferred that the on-line impregnation is suitable only for a low value of capacitance (1 μF, lesser diameter of wound element <80 mm). This is due to the slippage of film-foil during winding above 80 mm diameter and high mandrel speed (15RPM). It is noticed that the maximum resin is dripping out during winding itself at 5RPM. These developed capacitors are breaking down at lower voltage due to lesser amount of resin and non-uniform impregnation. Finally, a combined impregnation method is implemented. Firstly, resin dipped film-foil turns (diameter: 155 mm) are wound at 5RPM using on-line impregnation winding machine. Then, this partial resin filled wound capacitor is again impregnated with resin to fill the edges of film-foils as per the off-line impregnation method. So, it is confirmed that the on-line impregnation along with manual impregnation gives the best results in terms of high voltage holding capability, leakage current, and life.

Film-foil winding is performed under dehumidified environment and air laminar flow through high efficiency particulate air (HEPA) filter. Resin is degassed under rotary vacuum to release gases and water vapors for 4 h. Bubble free resin is ensured before processing in both on-line impregnation bath tub and second stage off-line (manual) impregnation. Resin is slowly filled in partially impregnated wound capacitor. Rotary vacuum is again applied for 6 h during off-line impregnation. The excess low viscosity resin fills the air pockets uniformly inside the capacitor element. Finally, metal discs are pressed from both sides against extended aluminum foils and curing is performed at 70 °C for 3 h.

IV. EXPERIMENTAL RESULTS

It is extremely important to apply 30% static electric field of the operating voltage across oil-free capacitors some time before full charging. This sweeps out mobile ionic species from capacitor and reduces the local electric field enhancement. Important parameters (4 μF, 10 kV) are experimentally measured as per below discussion.

A. Insulation resistance (IR)

Test voltage (10 kV) is applied for IR measurement between capacitor terminals.[11] Capacitor is left charged at 10 kV with solenoid actuated switch for a period of 5 min ± 5 s. Residual voltage left on the capacitor is measured after 5 min with a dc high voltage probe (1000 MΩ). Insulation resistance (R) is computed from the following formula:

$$R = t/\ [2.3 \times C \times \log(V1/V2)], \qquad (2)$$

where t = time in s, C = capacitance in μF, $V1$ = test voltage, $V2$ = residual voltage, and R = insulation resistance in MΩ.

Discharging resistance value is calculated as 670 MΩ for discharging time (300 s) and voltage drop from 10 kV to 8.94 kV. This equivalent resistance (670 MΩ) is a parallel combination of 1000 MΩ (HV probe resistance) and actual capacitor insulation resistance (IR). After a small calculation, the IR value is inferred as ≈2000 MΩ.

B. Leakage current

Oil-free capacitors are kept charged for 60 s to ensure handling of high voltage for an extended amount of time. Charging voltage is raised at 100 V/s rate. Leakage currents follow the power equation $\{I_L = a \times (V)^b\}$ with test voltage. Leakage current values are recorded only after reaching the capacitor voltage at steady state condition (>60 s). Leakage current (4 μA ± 1 μA) is measured at 10 kV dc voltage. This also confirms more than 2000 MΩ insulation resistance.

C. Life test

Eight capacitors (200 J) are developed and tested at 11 kV dc for 60 s. Capacitance values are as follows: 3.9, 3.95, 3.74, 3.85, 3.76, 3.84, 4.4, and 5 μF. Two capacitors are tested for 1000 shots. Charging voltage is raised at 100 V/s slope using constant current dc power supply. Dissipation factor is slightly changed from initial values of 0.0006 to 0.0008 and 0.0007. Change in capacitance values are less than 2% for both capacitors. These capacitors are healthy and holding a charging voltage of 10 kV for 60 s. Test results support good design and development process for high voltage, oil-free capacitors.

D. Measurement of the self inductance of the capacitors

Coaxial conductors are so designed for minimum spacing between "go" and "return" paths to ensure low inductance. However, it must be remembered that magnetic forces occur which will tend to separate the conductors unless adequately secured. Therefore, both spark gap and shorted coaxial load are mechanically secured using M3 screws and with internal threading on capacitor plate, respectively. Bottom disc of the cylindrical capacitor (5 μF) is connected with a solid rod of 40 mm diameter up to top ground electrode disc. This brings both terminals at one side with a small air gap to form a self break over spark gap. Capacitor is charged up to break over voltage (few kV). Discharging current waveform is measured using inductive sensor as shown in Figure 5. Self inductance (21 nH) is computed for hollow cylindrical capacitor (5 μF, 10 kV) with time period (2 μs) of current waveform. Inductance of a coaxial transmission line system is expressed as

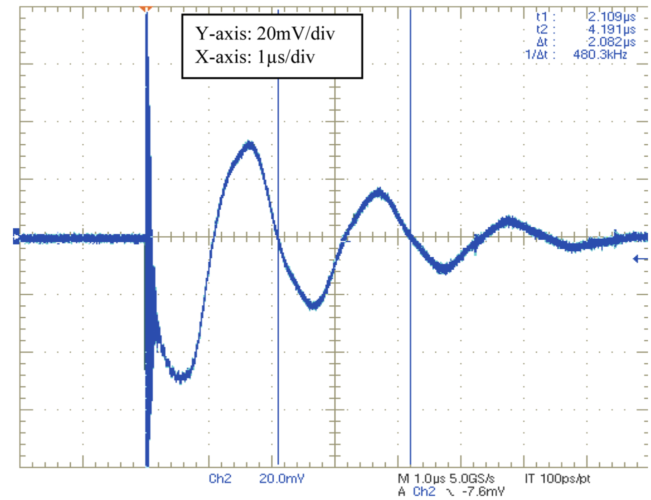

FIG. 5. Inductive pick up (T ≈ 2.0 μs) for inductance measurement of hollow cylindrical pulse capacitor 5 μF, 10 kV.

$$L = 2 \times Le \times \ln\left(\frac{OD}{ID}\right) \times 10^{-7} \text{in H}, \qquad (3)$$

where L = Inductance of the coaxial capacitor, OD = outer diameter of the coaxial line (mean diameter of the coaxial capacitor), ID = diameter of the solid aluminum rod as return path in same units, and Le = length of the capacitor in m.

Two capacitors are utilized as an energy module (400 J) for a PF device. Energy module (20 kV, 2.06 μF) is a series combination of two hollow cylindrical capacitors (4.4 μF and 3.9 μF). Compact experimental setup is shown in Figure 6, which consists of oil-free energy module, spark gap, and shorted coaxial load. This electrical circuit is mechanically designed to yield the lowest possible overall inductance. A mathematical formulation is carried out to find the total circuit inductance (70 nH) of this high voltage pulsed power setup as follows:

$$\text{Total circuit inductance}: \ 70\,\text{nH}\,(33\,\text{nH} + 37\text{nH}),$$
$$\text{Shorted coaxial load and spark gap}: \ 33\,\text{nH}$$
$$= (\ln(34/5) \times 2 \times 10^{-7} \times 0.074) + (\ln(16/10) \times 2 \times 10^{-7} \times 0.050),$$
$$\text{Two series capacitors}\,(2\,\mu\text{F},\ 20\,\text{kV}): \ 37\ \text{nH}.$$

Shorted coaxial electrical load is developed using aluminum hollow cup. A spark gap is developed between a load terminal and the capacitor high voltage central electrode. This load has similar geometry to the actual PF device. Self break over voltage can be varied by varying the length of the central pin electrode. This pin is located at the center of shorted aluminum cup load. Discharging shot is performed at 20 kV and under damped voltage waveform is stored in the digital storage oscilloscope to calculate the circuit inductance. Average time period and circuit inductance are inferred as 2.42 μs and 72 nH, respectively. This is close (<3%) to the mathematically calculated circuit inductance of 70 nH.

E. Development of PF device using oil-free capacitors

Actual PF device is fabricated as per electrical and mechanical parameters of the above assembled coaxial pulsed

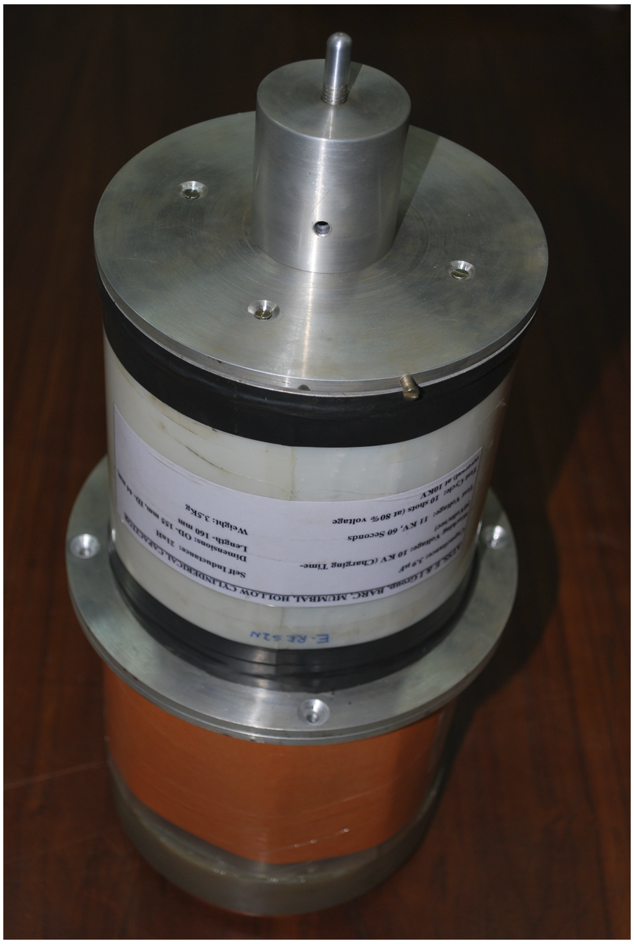

FIG. 6. Compact pulsed power system (20 kV, 400 J).

power system. This developed PF device is connected in place of a previous shorted load. Thirty shots (charging-discharging) are performed at 20 kV, 400 J. Current (not to scale), PF central electrode voltage, and capacitor discharging voltage waveforms are shown in Figure 7. Preliminary experiments

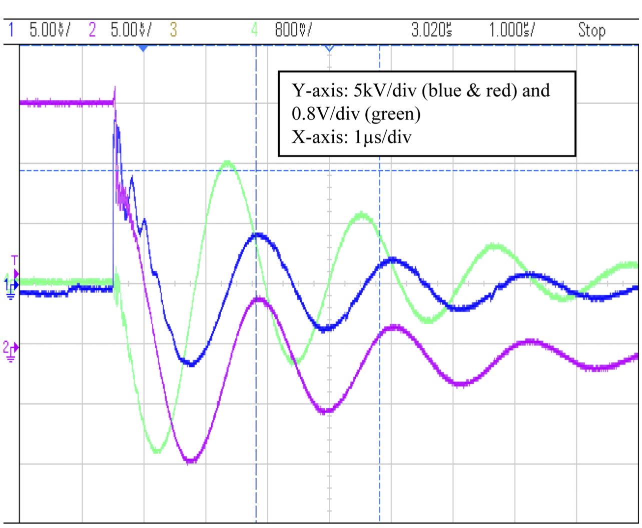

FIG. 7. Current (green), voltage on PF central electrode (blue), and capacitor discharging voltage (red) waveforms for capacitor energy module of 20 kV, 400 J with actual load of a PF device.

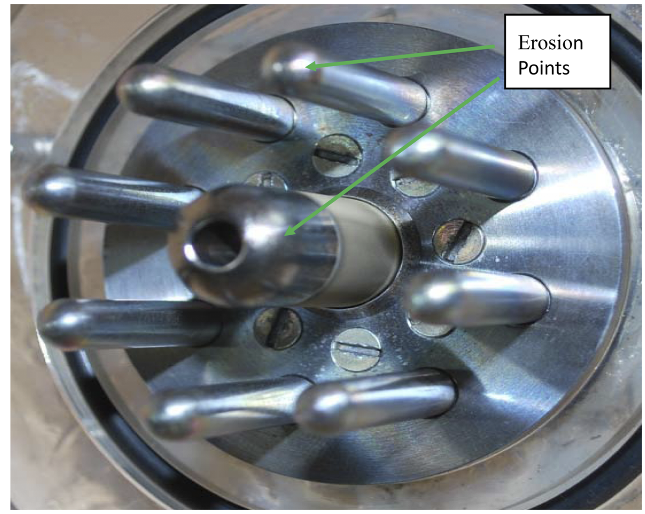

FIG. 8. PF electrode's erosion after a few tens of shots at 400 J, 20 kV.

are conducted by filling nitrogen gas at 1 mbar pressure inside the PF device. Discharging current peak value is calculated as ≈100 kA from ringing current waveform ($T_{avg.}$ = 2.14 μs, $L_{ckt.}$ = 56 nH, and Reversal factor = 0.67) as shown in Figure 7. Photograph of a assembled PF device (after thirty discharging shots at 400 J) is shown in Figure 8. Almost equal erosion at all the eight cathode pins and erosion at central electrode confirm good design of the PF device. These tests also examine the capability of the oil-free energy module and confirm the good design and development process of the hollow cylindrical capacitors. Availability of these oil-free capacitors is contributing to the introduction of new pulsed power applications in research and industrial systems never before feasible.

V. CONCLUSION

This paper has presented the efforts to develop compact, non-standard geometry, oil-free capacitors and successful utilization for a PF device (20 kV, 400 J). Oil-free capacitors often have higher capabilities with limited life than previous generation oil filled products.

Reduction in self inductance, weight, and volume is clearly observed from the below comparison of similar pulsed capacitor (data taken from website: General Atomic, Part No.: 37 636) as shown in Table I. The added advantage is of zero leakage due to oil-free (dry) design and non-standard hollow cylindrical geometry. The life of capacitor should be compared after consideration of effect of energy density, voltage reversal, current delivery, and single high energy module capability.

Electrolytic and oil-free, film-foil capacitor is compared for PF circuit parameters. Oil-free, PF device energy source parameters are 400 J, 20 kV, 100 kA, 56 nH, 0.075 J/cc in comparison to electrolytic capacitor bank[5] of 100 J, 5 kV, 59 kA, 45 nH, 0.052 J/cc. It is also inferred that the 75 J, 4.3 kV, 60 nH PF system[2] has higher circuit inductance compared to in-house developed system (400 J, 20 kV, 56 nH). This clearly shows the importance of advancement of oil-free capacitor technology in a less complex and costly manner.

TABLE I. Comparison of similar capacitors.

Make	General atomic (Maxwell) capacitor part no.: 37636	BARC, India lab
C (μF)	0.5	4
V (kV)	10	10
Ip (kA)	25	85
Energy (J)	25	200
ED (J/cc)	0.028	0.075
L (nH)	20	20
Size and weight	58 × 150 × 102 mm 1.3 kg (Rectangular)	ID: 44 mm, OD: 155 mm and L: 155 mm, 3 Kg (coaxial: hollow cylindrical)
Any comment	Standard rectangular geometry, Life > 10^8 shots @ 20% voltage reversal	Oil-free (solid), non-standard geometry (hollow cylindrical), Life > 1000 shots @ 80% voltage reversal

Flexibility of the compact oil-free PF system makes it useful for many applications where the orientation is an important factor.[12] Development of single capacitor (4 μF, 10 kV, 200 J) has definite advantages in comparison to many in parallel, such as improved reliability.[8] Discussed features make the oil-free (solid) capacitor an interesting energy module for high voltage, low inductance pulsed power systems.

VI. PROJECTION FOR THE FUTURE

The capacitors described for the most part represent the state of art development of oil-free, non-standard geometry pulsed power capacitors. The record of performance and parameters indicates decreasing volume of pulse capacitors year by year. Energy modules (oil-free, pulse discharge capacitor/bank) are very much in demand from tens of Joule to hundreds of Joule with enhanced voltage (tens of kV) for high energy pulsed power portable/mobile systems.

Future efforts will continue to develop oil-free capacitors with special features such as high current discharge and non-standard geometry.

ACKNOWLEDGMENTS

The authors are grateful to Shri Y. S. Mayya, Director, E&I Group, BARC for his continuous support and encouragement in development of this technology. The authors also acknowledge and thank Shri Satish G. Chavan and Shri Manohar A. Gurav, BARC Mumbai for their assistance at various stages of capacitor development and testing.

[1] S. S. Hussain, S. Ahmad, G. Murtaza, and M. Zakaullah, J. Appl. Phys. **106**, 023311 (2009).
[2] R. Shukla and A. Shyam, Rev. Sci. Instrum. **84**, 106112 (2013).
[3] W. J. Sarjeant, J. Zirnheld, and F. W. MacDougall, IEEE Trans. Plasma Sci. **26**, 5 (1998).
[4] P. Winsor IV, E. Lobo, M. Zafar, A. Munshi, and A. Ibrahim, in 28th Symposium for Passive Electronic Components, Carts USA, 2008.
[5] R. K. Rout, R. Niranjan, P. Mishra, R. Srivastava, A. M. Rawool, T. C. Kaushik, and S. C. Gupta, Rev. Sci. Instrum. **84**, 063503 (2013).
[6] L. Xiao, D. Huang, X. Deng, L. Yang, and L. Chen, J. Fusion Energy **34**, 699 (2015).
[7] R. A. Cooper, J. B. Ennis, F. W. MacDougall, and J. F. Bates, in *IEEE Pulsed Power Conference* (IEEE, 2001).
[8] S. K. H. Auluck, in *International Workshop and Expert Meeting of ICDMP* (IEEE, Warsaw, 2014).
[9] S. Qin and S. A. Boggs, IEEE Trans. Dielectr. Electr. Insul. **17**, 1298 (2010).
[10] R. K. Sharma, M. A. Gurav, and S. G. Chavan, in *IEEE 1st International Conference on Condition Assessment Techniques in Electrical Systems* (Catcon, 2013).
[11] IEEE, in *Indian Standard for Energy Storage Capacitors, 13666* (IEEE, 1993).
[12] R. Niranjan, R. K. Rout, R. Srivastava, T. C. Kaushik, and S. C. Gupta, Rev. Sci. Instrum. **87**, 033504 (2016).